sustainability

MDPI

Article

Optimizing the Informal-to-Formal Recycling Transition: A Multi-Objective Decision-Support Framework for Urban Waste Governance

Xianya Zeng [1], Tianyong Wu [2,*] and Jiantuan Hu [1,*]

[1] School of Management, Wuhan Institute of Technology, Wuhan 430205, China; 22506010074@stu.wit.edu.cn
[2] School of Environmental Science and Engineering, Hubei Polytechnic University, Huangshi 435003, China
* Correspondence: wutianyong@hbpu.edu.cn (T.W.); 19030701@wit.edu.cn (J.H.)

Abstract

The informal waste recycling sector provides livelihoods for roughly 0.2% of the urban population in developing economies, yet its formalization amid economic development creates trade-offs among social welfare, environmental performance, and fiscal sustainability. This study formulates the informal-to-formal recycling transition as a three-objective problem: minimizing the residual informal waste-picker headcount (an exit/displacement proxy rather than a measure of integration success), maximizing recycling rates, and minimizing government expenditure. We solve this problem with NSGA-II and SPEA2 on a stylized model whose parameters are calibrated for order-of-magnitude consistency with publicly documented Chinese municipal waste-management benchmarks, a directional sanity check rather than a formal parameter fit; each algorithm runs 30 times. SPEA2 attains a modestly higher hypervolume than NSGA-II (0.733 vs. 0.714; two-sided Mann–Whitney U rank test, $p \approx 3 \times 10^{-11}$), and both algorithms converge within roughly 50 generations on this tractable two-variable problem. An unconstrained random search remains highly competitive, underscoring how readily this low-dimensional frontier can be approximated. The decision space comprises two policy levers, the formalization target α and the enforcement intensity E; a subsidy dimension is excluded because it would enter the fiscal objective only as a cost without a benefit channel. All fiscal values are expressed in abstract model currency units. A one-at-a-time sensitivity analysis identifies the formalization gain coefficient γ_1 as the parameter with the highest hypervolume coefficient of variation (CV = 13.2%), pinpointing where empirical estimation effort matters most within this model. Scenario simulations under boom, recession, and transition conditions shift the Pareto frontier in distinct ways. A bi-objective ablation indicates that the three objectives are largely independent, since only a small share of bi-objective solutions is strictly dominated in the full three-objective space; a quantitative hidden-cost penalty is not established. A representative compromise strategy ($\alpha \approx 0.97$, $E \approx 0.33$) reaches a 44.5% recycling rate with near-complete formalization at modest fiscal cost. The framework thus serves as a transparent, reproducible decision-support tool for urban waste governance in developing economies, making explicit the trade-offs that the model implements.

Keywords: multi-objective evolutionary optimization; informal waste recycling; NSGA-II; SPEA2; urban sustainability; waste picker livelihood; Pareto frontier

Academic Editor: Cristina Trois

Received: 9 August 2026
Revised: 26 August 2026
Accepted: 31 August 2026
Published: 4 September 2026

1. Introduction

The informal-to-formal recycling transition in developing economies sits at the intersection of urban environmental management and household-level economic survival. Informal waste pickers recover a substantial share of urban recyclables at negligible public cost to the state, yet they operate outside formal regulatory, fiscal, and labor-protection frameworks. Economic development and municipal formalization policies progressively compress this operating space: as incomes rise, the opportunity cost of waste picking increases and labor moves toward formal employment, while mandatory waste-classification schemes and licensed recycling infrastructure displace unregulated collection networks. These dynamics create a structural tension in which the sector's environmental contribution and the livelihoods of its workers are coupled and potentially in conflict.

Policy choices in this transition impose hard trade-offs among social welfare, environmental performance, and fiscal sustainability. Formalization can raise recycling rates and reduce residual informal employment, but it requires public expenditure and risks displacing workers who lack alternative livelihoods. Because these objectives conflict, the transition is inherently a multi-objective problem, and single-objective analyses that scalarize the trade-offs into a weighted sum obscure the Pareto frontier of non-dominated alternatives available to policymakers. This study responds by formulating the transition as a three-objective optimization problem and developing a transparent, reproducible decision-support framework that makes these trade-offs explicit and searchable.

Four research questions structure the investigation:

- RQ1 (Modeling): How can the informal-to-formal recycling transition be formulated as a multi-objective optimization problem, and how do the two policy levers, the formalization target and the enforcement intensity, shape the trade-off among the social, environmental, and fiscal objectives?
- RQ2 (Algorithm): How do NSGA-II, SPEA2, and an unconstrained random search compare on this problem, and is evolutionary search necessary when the frontier is tractable in a low-dimensional decision space?
- RQ3 (Sensitivity and scenarios): Which model parameters dominate frontier uncertainty, and how do different macroeconomic conditions shift the Pareto frontier?
- RQ4 (Ablation and policy): Are the three objectives largely independent in this model, and which representative strategies balance them on the frontier?

The remainder of this paper is organized as follows. Section 2 reviews the related literature on informal waste recycling and on multi-objective optimization for urban sustainability, and situates the present contribution within it. Section 3 presents the three-objective model, its parameters, the optimization algorithms, and the experimental design. Section 4 reports the results organized around the four research questions. Section 5 discusses the methodological and policy implications, and Section 6 concludes.

2. Background and Related Work

The informal waste recycling sector constitutes one of the most visible yet under-quantified interfaces between urbanization, environmental management, and household-level economic survival. Across the developing world, an estimated 15–20 million people earn their livelihoods through informal waste picking and recycling activities [1], accounting for a median 0.2% of the urban population [1]. These figures, however, are estimates rather than censuses, and they conceal substantial definitional and measurement heterogeneity across countries. Reviews of the informal waste sector note that published headcounts are typically indicative estimates that are difficult to verify, and that reported totals vary with census year and geographical scope (a city core versus a metropolitan area) and often do not state whether they cover all informal workers or only specific activities such as dump picking [2]. Depending on the method and the reference population, global estimates range from roughly 12.5 to 56 million informal waste workers [2], while more recent conservative estimates place the global waste-picker population near 11.4 million [3]. The share of the working population engaged in waste picking likewise differs markedly across countries, from roughly 0.1–0.4% in several West African cities to about 0.7% in South Africa and 0.1% in India [4]. Country-level and global counts remain scarce because informal activity largely falls outside official statistics [4]. We, therefore, treat the global figure above as an order-of-magnitude reference rather than a precise measure. In China alone, research from the mid-2010s estimated 170,000–300,000 informal waste pickers operating in Beijing, recovering the large majority of the city's recyclables [5]. An earlier survey-based study documented that 72% of Beijing's 1.805 million tons of recyclable household solid waste was collected by informal channels, with approximately 22,800 curbside recyclers active across the city [6]. These workers form the upstream nodes of a vast but largely ungoverned recycling value chain that provides critical environmental services at negligible public cost. The quantitative importance of this contribution generalizes well beyond China: in Vietnam's Mekong Delta, informal collectors were shown to be essential to municipal solid waste management and circular-economy outcomes [7], and a comparative framework of Asian cities documented the substantial recycling volumes and municipal budget savings attributable to informal recovery in settings such as Delhi and Hanoi [8]. Household-level segregation and informal collection likewise underpin recycling performance in Dhaka [9].

However, the relationship between economic development and the informal recycling workforce is characterized by a structural tension. As GDP per capita rises, the opportunity cost of waste picking increases, pulling labor toward formal employment; simultaneously, municipal governments deploy waste classification policies and formal recycling infrastructure that compress the operational space of informal actors. The 2017 "National Sword" policy restricting waste imports, the 2019–2020 rollout of mandatory garbage sorting in Shanghai and Beijing, and the 2024 motorized tricycle licensing in Beijing collectively constitute a natural experiment in the rapid formalization of a sector that had previously absorbed surplus rural-to-urban migrant labor [5]. Steuer [10] analyzed the contesting dynamic between formal and informal collection systems in China, demonstrating that formal institutions have historically provided broad leeway that enabled informal collection to effectively solve urban waste management problems; this finding underscores the risk of hasty formalization undertaken without regard for system-level trade-offs. Yet formalization is not costless: it requires fiscal expenditure on subsidies and enforcement, risks displacing vulnerable populations who lack alternative livelihoods, and may paradoxically reduce total recycling rates if informal collection networks are dismantled faster than formal systems can scale [11]. Case evidence from Chinese secondary cities documents that recycling rates remain modest even after formal integration efforts, and that effective policy packages combine professional training, price advantages for formal channels, and information platforms, illustrating the practical complexity of the transition. Earlier economic modeling by Moreno-Sanchez et al. [12] demonstrated that integrating informal waste-pickers into a dynamic general equilibrium framework yields system-level efficiency through a complementary mix of taxes on virgin material and subsidies to material recovery, providing theoretical grounding for the policy instrument design problem explored here. The policy record from other developing regions reinforces the lesson that formalization must be designed with the workforce in mind. Grassroots waste-picker organizations in Brazil have advanced both recycling performance and progress toward the Sustainable Development Goals, illustrating the productive role formal cooperatives

https://doi.org/10.3390/su18179106

can play [13]. In Colombia, however, formalization has been hampered by persistent institutional and capacity barriers that limit waste pickers' effective integration into municipal policy [14], and comparative analysis of Bogotá and Lima highlights how the sequence of recognition, regulation, and integration shapes formalization outcomes [15]. More broadly, informal recyclers are now framed as stakeholders within circular-economy transitions whose inclusion requires deliberate policy design rather than automatic integration [16].

This transition involves competing objectives and is inherently a multi-objective optimization problem. In the framework presented here, formalization reduces the residual waste-picker population and raises the recycling rate up to a crowding-out threshold, while enforcement raises the recycling rate at a convex fiscal cost; a subsidy dimension is excluded, since it would enter the fiscal objective only as a cost with no benefit channel. The model does not endow formalization with a direct fiscal cost, and it does not track social protection or formal-employment outcomes, so the full livelihood–fiscal–environmental trilemma falls outside its scope. Classical single-objective approaches that scalarize these trade-offs into a weighted sum obscure the Pareto frontier and deprive policymakers of the full menu of non-dominated alternatives.

We emphasize a normative clarification at the outset: the objective of minimizing the waste-picker headcount (f_1) is not intended as advocating for the elimination of informal livelihoods, a position at odds with the substantial literature documenting waste pickers as essential environmental service providers [17,18] and the growing policy scholarship advocating for the inclusion of informal waste economies in municipal solid waste management frameworks [19]. Rather, f_1 is an *exit or displacement proxy*: the model assumes that workers displaced from informal recycling are absorbed out of the sector through rising economic opportunity, but it tracks only the residual headcount, not income, occupational safety, or social protection. A falling headcount should, therefore, be read as reduced residual informal employment, not as evidence of successful economic integration. We return to this normative issue in the Discussion.

Multi-objective evolutionary algorithms (MOEAs) have been extensively applied to urban sustainability problems, including land-use allocation [20], urban drainage design [21], sustainable development goal trade-offs at the city-system level [22], and municipal solid waste management, where MOEAs have been deployed for facility location-allocation [23] and waste-to-energy pathway selection [24]. The scope of MOEA applications in solid waste management has expanded considerably: robust multi-objective models address facility site-selection and capacity allocation [25], NSGA-II has been applied to municipal waste system design [26], and bi-objective metaheuristics, including NSGA-II and SPEA2 have been used for waste collection location-routing [27]. Recent work has also coupled multi-objective vehicle-routing with sustainable concerns for waste classification and collection, as in Shanghai [28]. In the broader evolutionary computation literature, MOEAs have also been applied to sustainable transitions [29]. Environmental-performance assessment of this kind is increasingly supported by recent quantitative work at the land and ecosystem level, e.g., coupling analyses of landscape ecological risk and ecosystem service value that link ecological status to regional planning [30]. Papalexopoulos [31] demonstrated that multi-objective optimization provides interpretable decision-support tools for public policy, particularly in domains where stakeholders hold disparate value judgments on efficiency–fairness trade-offs. Liu et al. [32] demonstrated that a bi-objective evolutionary framework could outperform greedy algorithms for migrant resettlement planning. The relevance of this agenda to the present journal is well established: *Sustainability* has published MOEA-based studies on municipal solid waste location–allocation [23] and waste-to-energy pathway selection [24], together with field case studies of source-separated collection [33]. These works, however, operate in settings where the waste-management system is already fully formal and the decision problem concerns infrastructure siting or process design. In contrast, the transition we model is characterized by the coexistence of a formal and an informal collection system, where the policy levers act on the displacement of an unregulated workforce whose livelihood and environmental contributions are coupled. To substantiate this claim, we conducted a structured keyword search in August 2026 across OpenAlex, Crossref, and major publisher platforms (ScienceDirect, MDPI, Springer, SSRN), with no publication-date restriction. Search strings crossed informal-sector terms such as "informal recycling", "informal sector", "waste picker(s)", "scavenger(s)", "catadores", and "recicladores" with formalization terms such as "formalization", "integration", and "transition" and algorithm terms such as "multi-objective optimization", "evolutionary algorithm", "NSGA-II", "SPEA2", "genetic algorithm", and "Pareto", queried at the title and abstract level. Of roughly 70 records title-screened, eight were assessed at the abstract level and four at the full-text level. All cross-block queries returned zero or irrelevant hits (e.g., "waste picker" AND "multi-objective": 0; "informal sector" AND "NSGA-II": 0; "catadores" AND "multi-objective": 0), and a recent review of MOEA applications in waste disposal systems [34] contains no coverage of the informal sector. The nearest neighbours identified are Shi et al. [35], who optimize formal e-waste collection networks with NSGA-II under exogenous informal-sector competition; Peña et al. [36], who solve a bi-objective routing problem embedding waste-picker behavior with an ant-colony metaheuristic and Kusi-Appiah et al. [37], who integrate informal pickers into a single-objective linear program. No study was found that applies MOEAs to the formalization transition itself, treating formalization and enforcement as decision levers and informal-sector outcomes as objectives. Subscription-only databases (Web of Science, Scopus) were not directly accessible; OpenAlex aggregates a substantial share of their indexed content, but coverage is not exhaustive. Turning to the Chinese empirical setting that anchors this study, recent quantitative assessments document the effects of the very policy interventions that define the formalization window. Evaluation of Shanghai's mandatory waste-classification rollout confirms substantial improvements in sorting compliance and recycling outcomes after 2019 [38]. The informal recycling system that these policies reshape is itself well characterized in the Chinese literature: Beijing's recyclable collection combines formal and informal channels, with informal scavengers and peddlers playing a central role in recovering materials such as PET bottles [39]. The environmental and social stakes of this system are most acute in the e-waste stream, where China's largely informal recycling sector has posed local environmental hazards even as it recovers valuable materials [40]. These studies, together with the benchmark figures in Section 3.7, situate the formalization transition in a densely studied empirical context while leaving the multi-objective decision problem that we address largely open.

This study addresses this gap by proposing a multi-objective evolutionary optimization framework for the informal-to-formal recycling transition. The contributions are threefold: (1) we formulate a three-objective optimization model of the informal-to-formal transition driven by two effective policy levers, the formalization target α and the enforcement intensity E, whose parameters are set to order-of-magnitude consistency with publicly documented Chinese municipal waste-management benchmarks through a directional sanity check rather than a formal fit; (2) we conduct a systematic experimental comparison of NSGA-II and SPEA2 on this problem, including global parameter sensitivity analysis (two-level factorial design), economic scenario simulation (boom, recession, transition), and bi-objective versus tri-objective ablation and (3) we identify representative candidate strategies on the Pareto frontier and characterize how the two modeled levers shape the trade-off surface. The framework is intended as a transparent, interpretable decision-support tool,

https://doi.org/10.3390/su18179106

and its structural simplicity—the search space solvable within 50 generations—is presented as a feature for policy accessibility rather than a limitation of algorithmic sophistication.

3. Materials and Methods

Figure 1 summarizes the step-by-step methodology of the framework. The pipeline proceeds from problem formulation, through parameter calibration, multi-objective optimization with three competing solvers, and performance metrics, to the experimental design whose results are reported in Section 4.

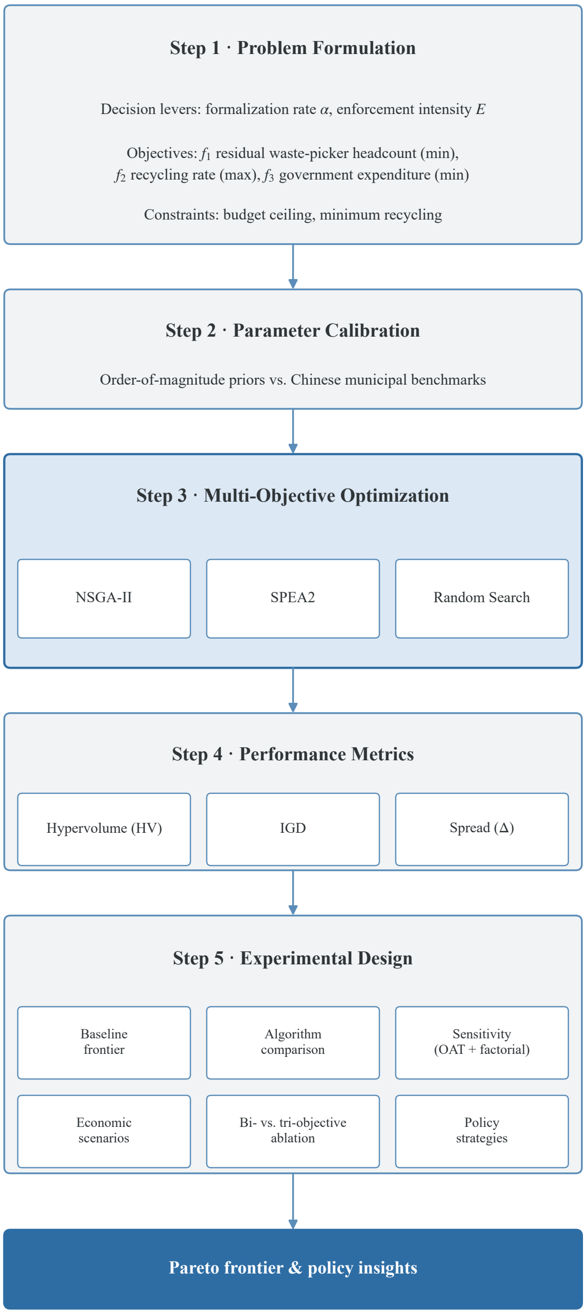

Figure 1. Step-by-step methodology of the multi-objective decision-support framework. The pipeline moves from problem formulation (decision levers, objectives, constraints), through parameter calibration against Chinese municipal benchmarks, multi-objective optimization (NSGA-II, SPEA2, random search), and performance metrics (HV, IGD, Spread), to the experimental design that produces the Pareto frontier and policy insights.

3.1. Problem Formulation

We model a generic megacity with population $P = 1 \times 10^7$, generating annual municipal solid waste W_{total} (tons/year). The city's recycling system is characterized by two continuous decision variables, which are the effective policy levers:

- $\alpha \in [0,1]$: the **formalization rate**, defined as the proportion of the recycling sector operated through formal (registered, regulated) entities rather than informal individual pickers.
- $E \in [0,1]$: the **enforcement intensity** of waste classification regulations, capturing the stringency of mandatory garbage sorting and the associated monitoring and penalty infrastructure.

These variables jointly determine the three objective functions and two constraints described below. The formalization target α is a policy setting the planner chooses directly rather than an outcome produced by enforcement; the model does not claim a causal channel from enforcement intensity to formalization. A subsidy dimension is excluded from the decision space: it would enter the fiscal objective only as a cost with no benefit channel, so it could never improve the frontier, and the model does not arbitrate subsidies against enforcement (Section 3.2.3). All fiscal quantities in the model are expressed in abstract model currency units (MU), not in a specific currency or price year.

3.2. Objective Functions and Constraints

3.2.1. Objective 1: Residual Waste-Picker Population (f_1, Minimize)

The residual informal waste-picker population is modeled as follows:

$$f_1(\alpha) = N_{\text{wp}}^{\text{base}} \cdot (1-\alpha) \cdot \exp\left(-\lambda \cdot \frac{\text{GDP}_{\text{per capita}}}{1000}\right) \tag{1}$$

where $N_{\text{wp}}^{\text{base}} = 20{,}000$ is the waste-picker stock *before* the absorption effect (0.2% of the urban population, following the global median reported in [1]), $\lambda = 0.5$ is the economic absorption elasticity, and $\text{GDP}_{\text{per capita}} = 8000$ (model currency units) is the reference per capita income level. The exponential term captures the structural pull of economic prosperity: at the reference income level, $\exp(-\lambda \cdot \text{GDP}_{\text{per capita}}/1000) = e^{-4} \approx 0.018$, so the residual headcount at zero formalization ($\alpha = 0$) is approximately 366 persons, not the pre-absorption stock of 20,000. Reported reductions are, therefore, measured against this $\alpha = 0$ counterfactual output (366 persons) under reference GDP, not against the pre-absorption stock; the bulk of the decline from 20,000 to the low hundreds is attributable to the fixed income term rather than to the formalization lever itself.

3.2.2. Objective 2: Recycling Rate (f_2, Maximize → Minimize Negative)

The total municipal solid waste recycling rate is modeled as a quadratic function of formalization and enforcement:

$$r(\alpha, E) = R_{\text{base}} + \gamma_1\alpha + \gamma_2 E - \gamma_3\alpha^2 \tag{2}$$

where $R_{\text{base}} = 0.26$ is the baseline recycling rate (typical for Chinese megacities in the absence of formalization-driven improvements), $\gamma_1 = 0.30$ captures the linear gain from formalization (standardized collection, economies of scale), $\gamma_2 = 0.25$ captures the gain from enforcement (compliance with source separation), and $\gamma_3 = 0.20$ captures the crowding-out effect: at very high formalization rates, the dismantling of informal collection networks may reduce marginal recycling gains. The recycling rate is clipped to $[0,1]$.

Since the optimization direction is minimization, we define the following:

$$f_2(\alpha, E) = -r(\alpha, E) \tag{3}$$

3.2.3. Objective 3: Government Expenditure (f_3, Minimize)

Total annual government expenditure is modeled as the cost of regulatory enforcement:

$$f_3(E) = C_{\text{enf}} \cdot E^2 \tag{4}$$

where $C_{\text{enf}} = 3 \times 10^8$ is the enforcement cost coefficient, in model currency units. The quadratic E^2 term reflects the convex cost of regulatory enforcement: stronger enforcement improves the recycling rate (through f_2) but at an increasing fiscal cost. All fiscal quantities are denominated in abstract model currency units rather than a specific currency or price year, so reported expenditure and budget values are comparable only within the model and should not be read as actual monetary amounts or shares of real GDP.

Two scoping properties bound the framework's claims. First, a subsidy dimension is excluded from the decision space because it has no benefit channel in the objectives: a positive subsidy would enter the fiscal objective only as a cost and improve neither f_1 nor f_2, so it could never appear on the Pareto frontier. The model, therefore, provides no evidence about whether subsidies outperform enforcement. Second, the model assigns no direct fiscal cost to formalization: f_3 depends on E alone. Both properties are revisited in the Limitations.

3.2.4. Constraints

Two inequality constraints ensure solution feasibility:

$$g_1: \quad f_3 - B_{\max} \le 0 \tag{5}$$

$$g_2: \quad R_{\text{base}} - r(\alpha, E) \le 0 \tag{6}$$

where $B_{\max} = 0.001 \cdot \text{GDP}_{\text{per capita}} \cdot P = 8 \times 10^7$ is the fiscal ceiling in model currency units, set to 0.1% of the model's reference income aggregate $\text{GDP}_{\text{per capita}} \cdot P$.

Note that the recycling constraint g_2 is redundant under the baseline parameters. Substituting Equation (2), g_2 requires $r \ge R_{\text{base}}$, i.e., $\gamma_1\alpha + \gamma_2 E - \gamma_3\alpha^2 \ge 0$. With $\gamma_1 = 0.30$, $\gamma_2 = 0.25$, $\gamma_3 = 0.20$ and $\alpha, E \in [0, 1]$, the left-hand side equals $\alpha(0.30 - 0.20\alpha) + 0.25E \ge 0.10\alpha \ge 0$, so the constraint is satisfied for every point in the decision space and excludes no candidate solution under the baseline. It would become binding only under parameter changes that make the non-baseline term $\gamma_1\alpha + \gamma_2 E - \gamma_3\alpha^2$ negative at some feasible decision point. More precisely, for $\gamma_2 \ge 0$ the constraint is relaxed over the whole decision space if and only if $\gamma_3 \le \gamma_1$; when $\gamma_3 > \gamma_1$, it binds in the lens-shaped region $\{\alpha > \gamma_1/\gamma_3,\ 0 \le E < (\gamma_3\alpha^2 - \gamma_1\alpha)/\gamma_2\}$ near $(\alpha = 1, E = 0)$. Under the baseline $\gamma_3 = 0.20 \le \gamma_1 = 0.30$, this threshold requires raising the crowding-out coefficient to more than 1.5 times its baseline value, or lowering γ_1 below γ_3. The sensitivity design in Section 4.3 does reach such points: at the OAT level $\gamma_1 \times 0.5$ and at the fractional-factorial corners with low γ_1 and high γ_3, g_2 excludes between 2.3% and 24.5% of the otherwise-feasible region, so the constraint is active in those parts of the model family even though it is inactive at the baseline calibration. Consequently, the baseline feasible region is determined entirely by the budget constraint g_1; g_2 is retained as a placeholder for a minimum-recycling requirement that is not active under the current calibration.

3.3. Parameter Calibration

Table 1 summarizes all model parameters, their baseline values, units, and literature sources. Parameters γ_1 through γ_3 and λ, C_{enf} are calibrated as order-of-magnitude priors, and their sensitivity is systematically assessed in Section 4.3. We emphasize that these parameters are not fitted to any municipality's data; they are set as transparent, order-of-magnitude priors chosen for consistency with publicly documented Chinese municipal waste-management benchmarks (Section 3.7). This choice has a direct methodological consequence: the model's outputs are directional and exploratory rather than point predictions, and any policy reading of the frontier must be interpreted as conditional on these priors. Empirical estimation of the parameters, in particular, the formalization gain coefficient γ_1, would require city-level panel data linking formalization interventions to observed recycling outcomes, which is outside the scope of the present modeling exercise and is identified in Section 4.3 and in the Limitations as the priority empirical task. The systematic sensitivity analysis is, therefore, not an optional complement but an integral part of the framework, since it delineates how far the qualitative results hold across the plausible prior range.

Table 1. Model parameters: baseline values and sources. All monetary quantities are in abstract model currency units (MU). A dash (—) indicates that the parameter is dimensionless.

Symbol	Meaning	Value	Unit	Source
P	City population	1.0×10^7	persons	Stylized megacity
$N_{\mathrm{wp}}^{\mathrm{base}}$	Baseline waste-picker stock	20,000	persons	[1]
R_{base}	Baseline recycling rate	0.26	—	Typical Chinese megacity
W_{total}	Annual MSW generation	3×10^6	t/yr	Typical megacity
$\mathrm{GDP}_{\mathrm{per\ capita}}$	Reference per capita income	8000	MU	Stylized reference
$B_{\max}$	Fiscal ceiling (0.1% of ref. income)	8×10^7	MU	Derived
λ	Econ. absorption elasticity	0.5	—	Calibrated prior
γ_1	Formalization linear gain	0.30	—	Prior
γ_2	Enforcement gain	0.25	—	Prior
γ_3	Crowding-out (quadratic)	0.20	—	Prior
C_{enf}	Enforcement cost coeff.	3×10^8	MU	Prior

3.4. Multi-Objective Evolutionary Algorithms

3.4.1. NSGA-II

The Non-dominated Sorting Genetic Algorithm II (NSGA-II) [41] is employed as the primary solver. NSGA-II uses non-dominated sorting to rank solutions into Pareto fronts, followed by crowding-distance computation within each front to maintain diversity. The algorithm configuration is as follows: population size 100, maximum generations 500, simulated binary crossover (SBX) with probability $p_c = 0.9$ and distribution index $\eta_c = 20$, polynomial mutation with per-variable probability $p_m = 1/2$ (i.e., $1/n_{\mathrm{var}}$ for the two-dimensional decision vector) and distribution index $\eta_m = 20$, and binary tournament selection. Real-valued encoding is used for the two-dimensional decision vector (α, E). Constraints are handled via pymoo's unified constraint-domination scheme (feasibility-first ranking by total constraint violation); infeasible solutions are retained and evolved rather than discarded.

3.4.2. SPEA2

The Strength Pareto Evolutionary Algorithm 2 (SPEA2) [42] is used as the comparison algorithm. Unlike NSGA-II, SPEA2 maintains an external archive of non-dominated solutions and uses a fine-grained fitness assignment scheme that accounts for both dominance strength and density. We configure SPEA2 with population size 100, archive size 100, and 500 generations, using the same crossover and mutation operators, initialization, random seeds, and constraint-handling scheme as NSGA-II for a fair comparison.

3.4.3. Random Search Baseline

A random search baseline samples 50,000 points uniformly from the decision space (100 points per "generation" over 500 iterations). These 50,000 draws constitute the total sampling budget, including infeasible draws. Each sampled point is first checked against the same feasibility constraints as the evolutionary algorithms; on average, roughly 25,900 samples per run (≈52%) are feasible, and only feasible samples are retained in the non-dominated archive. Because the two-variable decision space is small, the retained non-dominated archive typically grows to approximately 7000 points; we report metrics both for a fixed 100-point archive (matching the evolutionary population size) and for the complete non-dominated archive. This serves as a finite-budget random-search baseline; as shown in Section 4.2, it is highly competitive on this low-dimensional problem.

3.5. Performance Metrics

Three standard multi-objective performance metrics are employed:

- Hypervolume (HV): The volume of the objective space dominated by the obtained non-dominated set, bounded by a reference point set to 1.1× the maximum observed value in each objective across all runs. All three objectives are min–max normalized to $[0,1]$ before HV computation to ensure equal dimensional weighting [22].
- Inverted Generational Distance (IGD): The average Euclidean distance from each point in the reference Pareto set to the nearest point in the obtained approximation. The reference set is an empirical one, constructed as the non-dominated union of all solutions from all algorithms and all runs, and therefore, includes solutions produced by the algorithms being compared; consequently, IGD measures coverage of this jointly discovered region rather than independent convergence to the true Pareto front. IGD is computed on normalized coordinates. A sensitivity check against a reference front densely sampled from the decision space yields the same algorithm ranking.
- Spread (Δ): A simplified 1-D adaptation of Deb et al.'s (2002) [41] metric. The non-dominated front is sorted by f_1, and Δ is computed from consecutive Euclidean distances in the raw (un-normalized) objective space, with the first/last consecutive distances serving as the endpoint terms. Because this 3-D raw-coordinate variant is dominated by the f_3 scale, we report Δ only as a relative diversity comparison across algorithms rather than as an absolute diversity measure [41].

3.6. Experimental Design

Six experiments are conducted with heterogeneous replication structures that reflect their different inferential roles. Experiments 1, 2, and 4 use 30 independent runs per condition and support statistical inference; Experiment 3 uses fewer replicates per condition (5 for one-at-a-time, 3 for the fractional factorial) and reports descriptive coefficients of variation; Experiment 5 runs 30 replicates but summarizes a single descriptive dominance ratio over the non-dominated union, without per-run uncertainty and Experiment 6 is a deterministic post-processing selection of four knee points with no replication. In total, the study comprises 503 optimization runs. The per-experiment design is summarized as follows:

1. Baseline Pareto Frontier: NSGA-II (population 100, 500 generations) applied to the three-objective problem across 30 independent runs (seeds $1000 + i$) to generate the reference Pareto set and assess convergence behavior; results are aggregated as the non-dominated union across runs, with per-run hypervolume summarized as mean ± standard deviation.
2. Algorithm Comparison: NSGA-II, SPEA2, and Random Search compared across HV, IGD, Spread, and runtime, with 30 independent runs per algorithm (seeds $2000 + i + \text{hash}(\text{name}) \bmod 1000$). Two-sided Mann–Whitney U rank tests with Cliff's delta effect sizes are reported for HV, IGD, and Spread across algorithm pairs, using per-run values as the unit of analysis.

3. Parameter Sensitivity: Each of the five key parameters (γ_1, γ_2, γ_3, λ, C_{enf}) is varied one-at-a-time (OAT) at five levels ($\times[0.5, 0.75, 1.0, 1.25, 1.5]$ of baseline), with NSGA-II (population 100, 300 generations, 5 replicates per level, 125 runs total; seeds $3000 + \text{step} \cdot 10 + \text{rep}$). A 2^{5-1} fractional factorial (16 design points, 3 replicates each, 48 runs) complements the OAT analysis by estimating main effects. HV is computed under a local-baseline reference point (Section 4.3); the coefficient of variation (CV) of HV across the five levels quantifies the sensitivity of each parameter over the examined range. OAT and fractional-factorial results are descriptive summaries (CV and main effects), not inferential tests.
4. Economic Scenario Simulation: Three macroeconomic scenarios are simulated by adjusting λ and R_{base}: (a) *Boom* ($\lambda = 0.08$, $R_{\text{base}} = 0.30$), (b) *Recession* ($\lambda = 0.02$, $R_{\text{base}} = 0.20$), and (c) *Transition* with mandatory waste classification ($\lambda = 0.05$, $R_{\text{base}} = 0.28$, $E \geq 0.4$). Each scenario is run 30 times (NSGA-II, population 100, 500 generations; seeds $4000/5000/6000 + i$); each scenario's frontier is the non-dominated union across its runs, with hypervolume summarized as mean $\pm$ standard deviation.
5. Bi-Objective vs. Tri-Objective Ablation: Three bi-objective subproblems (f_1–f_2, f_1–f_3, f_2–f_3) and a tri-objective reference are each optimized over 30 independent runs (NSGA-II, population 100, 300 generations; seeds $7000 + \text{hash}(\text{name}) \bmod 500 + i$). The reported strictly-dominated shares are computed on the non-dominated union across runs and are single descriptive summary values without per-run uncertainty.
6. Representative Policy Strategies: Four representative candidate points are selected from the tri-objective Pareto frontier to illustrate the trade-offs among objectives: (A) complete formalization with high enforcement, (B) a gradualist point retaining a larger informal component, (C) minimum government expenditure, and (D) a compromise point chosen by the authors to illustrate a middle-ground allocation. This is a deterministic post-processing selection from the aggregated baseline frontier and involves no additional optimization runs or replication.

All experiments are implemented in Python 3.10.20 using the `pymoo` framework (v0.6.1.1) [43], NumPy 1.26.4, and SciPy 1.13.1, and are run single-threaded on an AMD Ryzen AI 9 H 465 processor (20 logical cores, Windows 10). Wall-clock runtime is measured with `time.perf_counter()` around the optimization loop only, excluding metric computation, plotting, and I/O. Because random search has no evolutionary operators, its lower runtime reflects a lighter pipeline rather than a direct efficiency advantage; runtime is reported as a descriptive indicator of computational footprint, not as a strict efficiency comparison. Source code and the per-run numeric outputs of all optimization runs are provided in the Supplementary Materials.

3.7. Directional Order-of-Magnitude Check: Chinese Municipal Benchmarks

As a directional order-of-magnitude check rather than a formal calibration, we compare the stylized model's scale parameters against publicly available Chinese municipal benchmarks. For Beijing (population $\approx$ 21.8 million), annual MSW generation has been reported at approximately 9.0×10^6 tons [44], of which the formal municipal system processed on the order of 6.7 million tons in an earlier year (2011) [5]. The implied informal-sector residual is, therefore, roughly $9.0 - 6.7 \approx 2.3$ million tons. Because the two figures come from different statistical years and accounting scopes, however, this difference is a quantity-of-magnitude reference only and should not be read as a precisely measured informal throughput. The informal recycling workforce in Beijing was estimated at 170,000–300,000 persons during the mid-2010s peak [5,10], before the national waste-classification mandate (2019–2020 rollout) and the subsequent motorized-tricycle restrictions (2024); informal channels recover the large majority of the city's recyclables [5], and recycling rates achieved primarily through informal collection in Chinese cities are reported in the range of roughly 17–38% of municipal solid waste [45]. These figures anchor only the order of magnitude of the model's parameters; they are not fitted values.

For the stylized megacity used throughout the model ($P = 1 \times 10^7$, comparable in scale to a large Chinese metropolis), the scale parameters are set as independent stylized values rather than as strict linear scalings of the Beijing figures. The baseline waste-picker stock $N_{\mathrm{wp}}^{\mathrm{base}} = 20{,}000$ follows the 0.2% of urban population median rule [1] ($0.002 \times 10^7 = 20{,}000$), not a scaling of Beijing's 170,000–300,000 mid-2010s workforce (which would yield roughly 78,000–138,000 at the population ratio). Annual MSW generation $W_{\mathrm{total}} = 3 \times 10^6$ tons/year is likewise an independent stylized value, within the plausible range for a city of this size (a population-ratio scaling of Beijing's 9.0 Mt would give ≈ 4.1 Mt). The baseline recycling rate $R_{\mathrm{base}} = 0.26$ sits within the 17–38% range observed for informal-channel recycling in Chinese cities [45]. The model's predicted recycling rate under the representative compromise strategy (D) (44.5%) is directionally consistent with the improvements observed in Chinese cities that implemented mandatory classification (e.g., Shanghai's rate rose from approximately 20% to over 35% within two years of implementation). This comparison serves as a sanity check on the direction and magnitude of the results, not as a formal parameter estimation; we stress that the model is not fitted to Beijing or any other city's data but is designed to produce order-of-magnitude consistency with empirically documented benchmarks. Because the check compares relative quantities (recycling rates and parameter magnitudes) rather than the model's absolute scale, the stylized population $P = 1 \times 10^7$ need not equal Beijing's 21.8×10^6 for the order-of-magnitude consistency claim to hold; the same benchmark figures support the stylized city, which lies within the plausible size range of large Chinese metropolises (Section 3.7). The population scaling would affect the model's absolute headcount and throughput, but not the direction or relative magnitude of the transition outcomes reported here.

4. Results

4.1. Baseline Pareto Frontier

Figure 2 presents the Pareto frontier obtained by NSGA-II, comprising 2544 non-dominated solutions aggregated across 30 independent runs. The frontier spans $\alpha \in [0.69, 1.00]$ and $E \in [0.00, 0.52]$, corresponding to objective ranges of $f_1 \in [0, 113]$ persons, $f_2 \in [-0.50, -0.36]$ (equivalently, a positive recycling rate $r = -f_2$ over $[0.36, 0.50]$, i.e., 36–50%), and $f_3 \in [0, 8.0 \times 10^7]$ model units (the fiscal ceiling, since $f_3 \leq B_{\max} = 8 \times 10^7$). As discussed in Section 3.2.4, the recycling constraint g_2 is redundant under the baseline parameters, so the fiscal ceiling g_1 alone bounds this frontier's decision region.

To characterize the shape of the aggregated Pareto frontier (30 runs, $n = 2544$ non-dominated points), we report Spearman rank correlations among the positive recycling rate $r = -f_2 \in [0.36, 0.50]$ (i.e., 36–50%), the residual headcount f_1, and government expenditure f_3. The recycling rate and government expenditure are nearly monotone on the frontier ($\rho_{r,f_3} = +0.99$), while both are weakly positively correlated with f_1 ($\rho_{r,f_1} = +0.21$, $\rho_{f_1,f_3} = +0.13$). These values are descriptive geometric summaries of the jointly discovered frontier rather than inferential tests, since the aggregated points are not independent samples (they are drawn from 30 optimization runs); no point-level p-values are reported. The Pareto frontier is concave toward the ideal point, consistent with convex trade-off surfaces commonly observed in resource-allocation optimization problems.

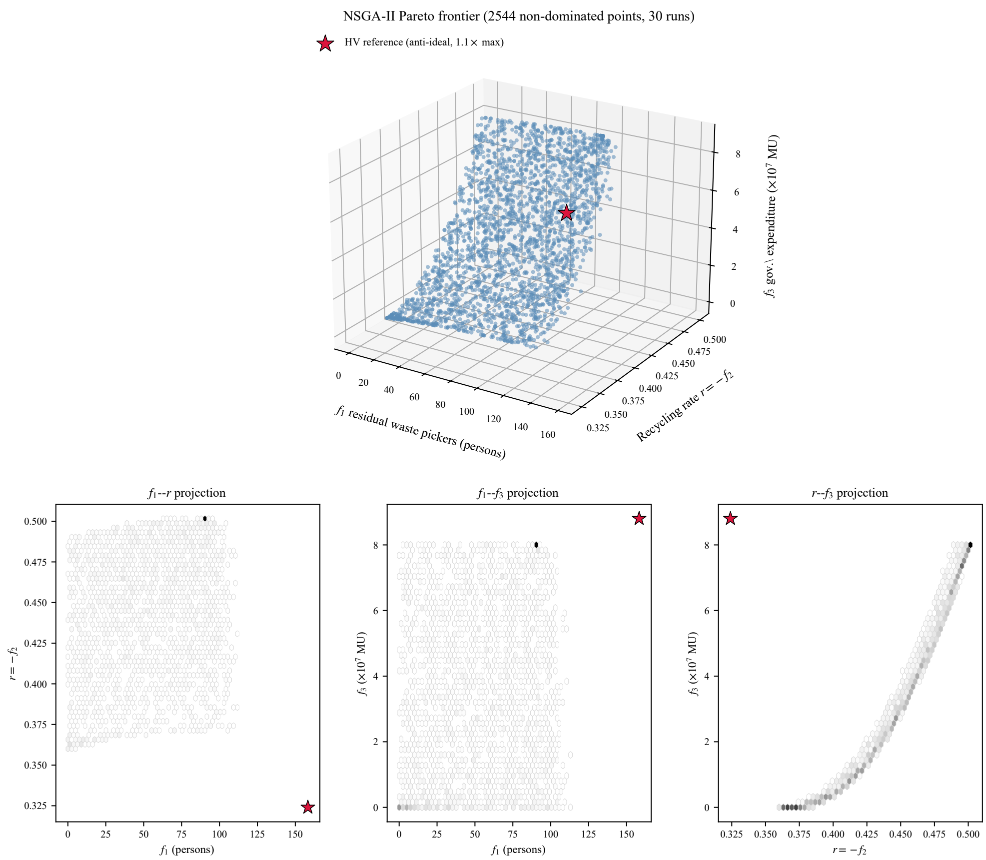

Figure 2. Three-dimensional Pareto frontier obtained by NSGA-II. The surface comprises 2544 non-dominated points aggregated from 30 independent runs, colored with a single neutral shade so that the third objective f_3 is encoded by the vertical axis alone. Lower sub-figures show 2D density projections onto the f_1–f_2, f_1–f_3, and f_2–f_3 planes, where shading reflects point density rather than objective values. The red star marks the hypervolume reference point, an anti-ideal point at 1.1× the maximum of each objective, which bounds the dominated region for the hypervolume computation.

Convergence analysis reveals that NSGA-II reaches a stable HV plateau within approximately 50 generations (final HV $= 0.714 \pm 0.007$, normalized, full-caliber reference), suggesting that the problem's two-variable search space is sufficiently tractable for a population of 100 to saturate quickly. The Random Search curve reports the cumulative-archive hypervolume and is monotone non-decreasing by construction, converging to the full-caliber terminal value reported in Table 2 and Figure 3 (Random-full 0.758 ± 0.0004).

Table 2. Algorithm performance comparison on the normalized objectives (mean ± standard deviation, 30 independent runs). Random@100 uses a fixed archive of 100 points, matching the population size of the evolutionary algorithms; Random-full retains the complete non-dominated archive. Bold entries indicate the best value for each metric. Pairwise comparisons use two-sided Mann–Whitney U tests with Holm–Bonferroni correction (six pairs per metric) and Cliff's δ effect sizes (Section 3.5); see Section 4.2 for the detailed test results. Runtime is a descriptive computational-footprint indicator (the random-search pipeline is lighter), not a strict efficiency comparison.

Metric	NSGA-II	SPEA2	Random@100	Random-Full
HV (normalized)	0.714 ± 0.005	0.733 ± 0.005	0.731 ± 0.010	$\mathbf{0.758 \pm 0.0004}$
IGD (normalized)	0.062 ± 0.003	0.072 ± 0.006	—	$\mathbf{0.0055 \pm 0.0013}$
Spread (Δ)	0.672 ± 0.060	$\mathbf{0.623 \pm 0.040}$	—	0.654 ± 0.005
Runtime (s)	2.95 ± 0.10	6.62 ± 0.20	—	3.73 ± 0.05
Archive size	100	100	100	≈7000

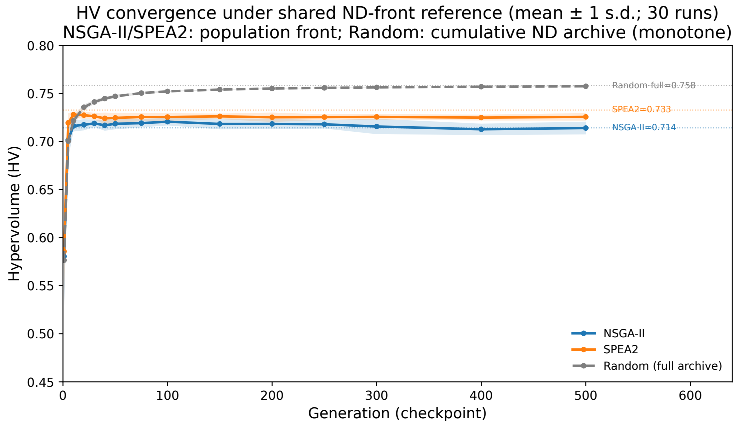

Figure 3. Hypervolume convergence curves (mean ± 1 SD across 30 runs), computed with the same shared reference point and a fixed normalization basis as Table 2. NSGA-II (blue) and SPEA2 (orange) show the hypervolume of their current feasible non-dominated population at each checkpoint, whereas Random Search (gray dashed) shows the hypervolume of its cumulative non-dominated archive (full-caliber, monotone non-decreasing). Dashed reference lines mark the corresponding full-caliber terminal values from Table 2. Both evolutionary algorithms plateau within approximately 50 generations.

4.2. Algorithm Comparison

SPEA2 attains a significantly higher HV distribution than NSGA-II (Mann–Whitney $U = 900$, $p = 1.8 \times 10^{-10}$ after Holm–Bonferroni correction across six pairwise tests; Cliff's $\delta = +1.00$, large effect; median 0.731 vs. 0.715) and a lower (better) Spread (median 0.621 vs. 0.668, $\delta = -0.51$, large effect). However, SPEA2 attains a significantly worse IGD than NSGA-II (median 0.072 vs. 0.062, $\delta = +0.85$, large effect), indicating that its front is less close to the shared reference Pareto despite covering more hypervolume. The two evolutionary algorithms run in comparable wall-clock time (≈25 s per run).

Random search is highly competitive with the evolutionary algorithms on this problem. With a fixed archive of 100 points (matching the population size), Random@100 attains an HV of 0.731 ± 0.010, statistically indistinguishable from SPEA2 and significantly higher than NSGA-II. When allowed to retain its complete non-dominated archive, Random-full reaches an HV of 0.758 and an IGD of 0.0055, outperforming both evolutionary algorithms. This is not an artifact of archive truncation: capping the random archive to 120 points lowers its HV by about 0.02 (0.759 to 0.740). Instead, it reflects a structural property of this problem. The two-variable decision space (α, E) is small, smooth, and convex, and the random search's 50,000 samples yield roughly 7000 non-dominated points, densely covering the Pareto surface that the population-100 evolutionary algorithms approximate with only 100 points. The apparent advantage of evolutionary search is thus a consequence of the archive cardinality asymmetry rather than of algorithmic search power. This has positive implications for policy users, who can reach near-optimal frontiers with simple uniform sampling on this low-dimensional problem, while the evolutionary algorithms remain valuable as the scalable approach when the decision space grows.

Table 2 summarizes the comparative performance of the three algorithms across all metrics, and Figure 4 visualizes the corresponding per-run distributions of HV, IGD, and Spread.

4.3. Parameter Sensitivity

Figure 5 presents the sensitivity heatmap and the coefficient of variation (CV) of HV for each parameter. Each of the five parameters is varied one-at-a-time across five multiplicative levels ($\times[0.5, 0.75, 1.0, 1.25, 1.5]$ of baseline) with five replicates per level (NSGA-II, population 100, 300 generations). HV is computed under a local-baseline reference point, so its absolute values are not directly comparable to Table 2, but the CV ranking is invariant to the normalization choice.

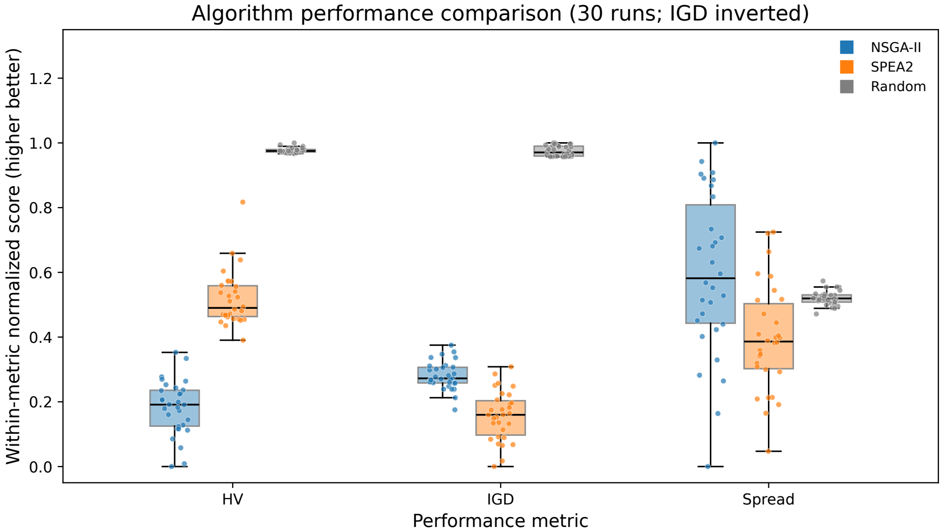

Figure 4. Multi-metric algorithm comparison (3 × 3 grid). Rows: hypervolume, inverted generational distance, and spread. Columns: NSGA-II, SPEA2, and Random Search. Boxplots summarize 30 independent runs with overlaid swarm plots. The random search column shows the Random-full configuration (complete non-dominated archive); the Random@100 configuration (fixed archive of 100 points, matching the evolutionary population size) is reported in Table 2 but is not shown here.

Over the examined one-at-a-time ranges, the formalization gain coefficient γ_1 exhibits the highest coefficient of variation of HV (CV = 13.2%), followed by the crowding-out coefficient γ_3 (CV = 7.6%), the enforcement gain γ_2 (CV = 4.0%), the enforcement cost coefficient C_{enf} (CV = 2.1%), and the economic absorption elasticity λ (CV = 1.4%).

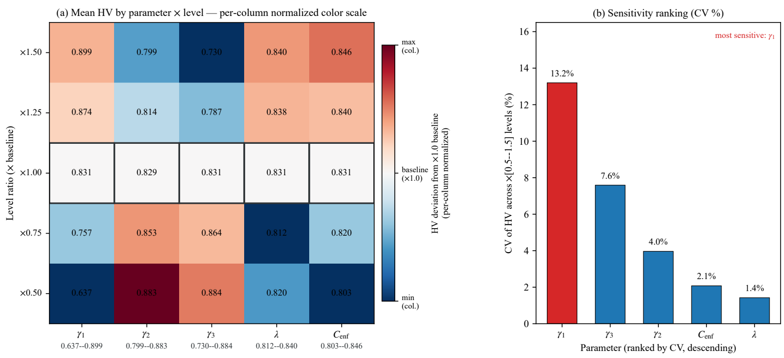

Figure 5. Parameter sensitivity analysis (one-at-a-time, five multiplicative levels $\times[0.5, 1.5]$ of baseline, five replicates per level). Left: heatmap of mean hypervolume for each parameter at each level. Because the parameters differ widely in dynamic range, the heatmap color scale is normalized independently within each parameter column, so column shading reflects within-parameter sensitivity and colors are not directly comparable across columns; the actual HV range of each column is annotated below the corresponding label, and the baseline level is outlined. Right: coefficient of variation (CV, %) ranking across parameters. HV is computed under a local-baseline reference point; absolute values are not directly comparable to Table 2, but the CV ranking is invariant to the normalization choice.

The relatively high sensitivity of γ_1 within the examined range indicates that the marginal environmental return on formalization is a consequential modeling assumption: if γ_1 is overestimated, the Pareto frontier will overstate the recycling gains achievable at a given fiscal cost, potentially misleading policy design; conversely, underestimating γ_1 may under-prescribe formalization. The relatively low sensitivity of λ and C_{enf} suggests that, within the explored ranges, the qualitative structure of the Pareto frontier is robust to uncertainty in these parameters.

A monotonic decreasing trend is observed for γ_2 (enforcement gain): HV decreases as γ_2 increases across the explored range (from 0.883 at $\times 0.5$ to 0.799 at $\times 1.5$). We report this as an empirical observation within the examined range and flag it for closer sensitivity decomposition rather than attributing it to a single mechanism.

4.4. Economic Scenario Analysis

Measured with a shared anti-ideal reference point and a shared normalization basis across all three scenarios, the boom scenario produces the largest normalized hypervolume (HV $= 0.764$), followed by the transition scenario (HV $= 0.366$) and the recession scenario (HV $= 0.218$). This ordering is consistent with the analytic dominance structure of the model: for any identical (α, E), the boom scenario ($\lambda = 0.08$, $R_{\text{base}} = 0.30$) yields a lower residual headcount f_1 and a higher recycling rate than the transition scenario ($\lambda = 0.05$, $R_{\text{base}} = 0.28$) at equal fiscal cost f_3, and its feasible region is strictly larger (no $E \geq 0.4$ floor). Hypervolume here measures objective-space coverage under a common definition; it does not indicate that any scenario's feasible *decision* space is larger.

The recession scenario exhibits a systematic shift toward larger waste-picker populations and lower recycling rates, consistent with the dual mechanism of reduced labor-market absorption ($\lambda = 0.02$) and reduced consumption-driven recyclable waste generation ($R_{\text{base}} = 0.20$). This shift can be interpreted as an increase in "social pressure": the Pareto frontier moves into regions where achieving a given recycling performance requires either higher expenditure or tolerance of larger informal populations.

Figure 6 overlays the Pareto frontiers under three economic scenarios.

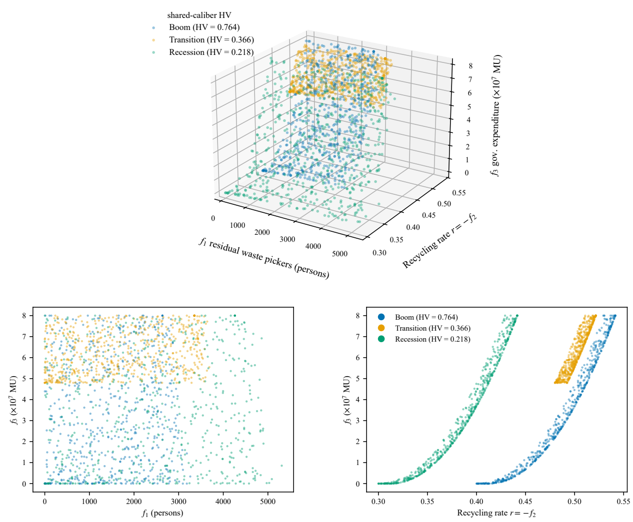

Figure 6. Pareto frontiers under three macroeconomic scenarios, shown on a common set of axes. The three scenarios are distinguished by color (blue: boom; orange: transition; teal: recession), and two lower panels show the f_1–f_3 and f_2–f_3 projections of the same frontiers to support reading of the three-dimensional structure. The third axis labels government expenditure f_3 in model currency units ($\times 10^7$ MU). Scenario hypervolumes are computed with a shared anti-ideal reference point ($1.1\times$ the maximum of each objective over the shared non-dominated union of all three scenarios) and a shared normalization basis; under this common-caliber definition, the boom scenario attains the largest normalized hypervolume (HV $= 0.764$), followed by transition (HV $= 0.366$) and recession (HV $= 0.218$).

4.5. Bi-Objective Versus Tri-Objective Optimization

The proportion of bi-objective solutions that are strictly dominated in the three-objective space is low across all three ablations (0.00–0.56%), indicating that the three objectives are largely independent in this model. For each ablation, the solutions reported are the constraint-filtered, nondominated set of each run's final population, pooled across the 30 runs and made nondominated in the retained objectives; the dominance share is reported as a descriptive statistic without a threshold or significance test. This dominance share describes the current approximate solution sets only; it does not by itself quantify the hidden cost of omitting an objective, because a bi-objective optimizer is free to push any objective that is neutral to the retained objectives to its boundary. For instance, when fiscal cost (f_3) is omitted, the enforcement lever E still enters the recycling rate via $\gamma_2 E$ but carries no cost penalty, so bi-objective solutions drive E toward the budget ceiling and the resulting expenditure concentrates near the upper bound. This concentration is an artifact of the missing cost signal rather than an inevitable penalty of two-objective optimization. Establishing a well-defined implicit penalty would require a reproducible pairing or aggregation rule that does not depend on sampling density; we do not claim such a rule here.

These results, therefore, do not establish a quantitative hidden-cost penalty or a necessity argument for tri-objective optimization; they support the weaker claim that the objectives are largely independent, so that a policy recommendation should be drawn from the full three-objective trade-off rather than from a reduced two-objective view. Table 3 and Figure 7 report the dominance analysis for the three bi-objective ablations.

Table 3. Bi-objective versus tri-objective ablation results: percentage of bi-objective solutions that are strictly dominated in the full three-objective space. Values are descriptive; no threshold or significance test is applied.

Omitted Obj.	Dominated (%)	Bi-Objective Solutions
f_3 (fiscal cost)	0.00	2621
f_2 (recycling rate)	0.00	12
f_1 (waste pickers)	0.56	2305

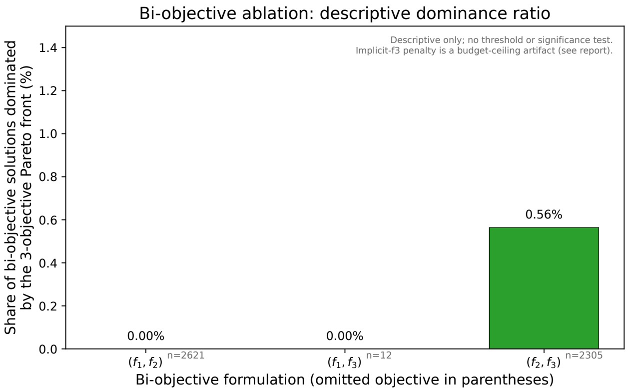

Figure 7. Dominance analysis of bi-objective versus tri-objective optimization. Bars show the percentage of bi-objective solutions strictly dominated in the full three-objective space; values are descriptive only, with no threshold or significance test, and sample sizes are annotated above each bar.

4.6. Representative Policy Strategies

The compromise strategy (D) combines a formalization rate of 97% with an enforcement intensity of 0.33. Under this configuration, the residual informal headcount is reduced to 13 persons, measured against the $\alpha = 0$ counterfactual baseline of approximately 366 persons at reference GDP (Equation (1)); the pre-absorption stock of 20,000 is reduced by the fixed income term before any policy lever acts, so comparing 20,000 directly with 13 would misstate the policy contribution. The recycling rate reaches 44.5% (versus the 26% baseline), and annual government expenditure is 3.21×10^7 model units. We emphasize that strategy D is a representative compromise point chosen by the authors to illustrate a middle-ground allocation, not the output of a formal knee-point selection algorithm. Its representativeness is supported by its location in the region of highest curvature of the concave Pareto frontier, where the recycling rate gains begin to saturate relative to the fiscal cost, so it reflects the trade-off structure of the problem rather than an arbitrary pick. Nevertheless, an explicit, automated knee-point detection (e.g., a maximum-curvature or trade-off-ratio criterion applied to the discretized frontier) would make the selection reproducible and is identified as a worthwhile extension in the Future Research Directions; we retain the author-chosen point here for transparency.

Strategy C sets $E = 0$ and, therefore, carries zero fiscal cost, achieving complete formalization but a lower recycling rate of 36.0%. Strategy A drives $\alpha = 1.0$ and $E = 0.50$, achieving complete formalization and a recycling rate of 48.6%, at about 2.4 times the fiscal cost of strategy D. Strategy B retains a larger informal component ($\alpha = 0.73$, 98 residual pickers) at a recycling rate of 45.3%, representing a more gradualist approach.

The low fiscal cost of near-complete formalization reflects the model's assumption that formalization itself carries no direct expenditure; fiscal cost enters the framework only through the enforcement dimension. A subsidy dimension is excluded (Section 3.2.3), so these strategies carry no subsidy and the model does not compare subsidies against enforcement. Table 4 and Figure 8 present the decision-variable values and objective outcomes for four representative points on the tri-objective Pareto frontier.

Table 4. Representative policy strategies extracted from the Pareto frontier.

Strategy	α	E	f_1	Rec. Rate (%)	f_3 (10^7)
A: Min. pickers	1.00	0.50	0	48.6	7.63
B: Gradualist	0.73	0.32	98	45.3	3.14
C: Min. cost	1.00	0.00	0	36.0	≈ 0
D: Compromise	0.97	0.33	13	44.5	3.21

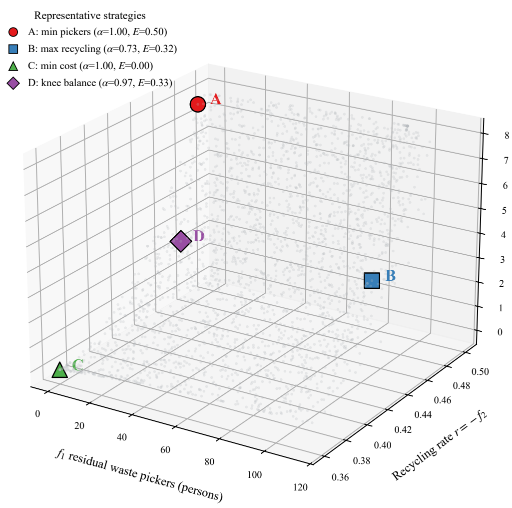

Figure 8. Representative candidate strategies selected from the tri-objective Pareto frontier: A ($\alpha = 1.00$, $E = 0.50$), B ($\alpha = 0.73$, $E = 0.32$), C ($\alpha = 1.00$, $E = 0.00$), and D ($\alpha = 0.97$, $E = 0.33$), a compromise point chosen by the authors to illustrate a middle-ground allocation. The four strategies are highlighted on the frontier with distinct colors and symbols (A: red circle; B: blue square; C: green triangle; D: purple diamond), while the underlying frontier is shown as a semi-transparent point cloud for readability. Strategy D achieves a recycling rate of 44.5% at $f_3 = 3.21 \times 10^7$ model units.

5. Discussion

5.1. Methodological Contributions

This study demonstrates that multi-objective evolutionary optimization provides a principled framework for analyzing the informal-to-formal recycling transition. On this stylized three-variable model and under the current configuration, SPEA2 attains a more evenly spread frontier (Table 2), which is relevant for policy applications where decision-makers benefit from a diverse menu of well-distributed alternatives rather than a cluster of near-identical solutions. This per-metric, configuration-specific result is consistent with SPEA2's archive-based diversity maintenance, but it should not be generalized into a default-algorithm recommendation for urban governance problems of moderate dimensionality without additional representative benchmarks.

At the same time, the competitive performance of random search on this two-variable problem warrants an explicit caveat about where the value of evolutionary search lies. Because the decision space is low-dimensional and the frontier smooth and convex, an unconstrained random search densely covers the Pareto surface (several thousand non-dominated points) and attains a hypervolume comparable to or better than the population-100 evolutionary algorithms; when the random archive is capped at the same cardinality as the evolutionary population, it remains statistically indistinguishable from SPEA2 on HV ($p = 0.061$ after correction). On Spread, however, SPEA2 remains significantly better than even the full random archive (median 0.621 vs. 0.653, $p = 1.4 \times 10^{-3}$ after correction). This reflects the problem's structural simplicity rather than a failure of the algorithms. The practical value of the evolutionary algorithms, therefore, lies in their scalability and in their ability to explore larger or constrained decision spaces, where uniform sampling becomes prohibitively inefficient. On the present low-dimensional benchmark, random search is a legitimate and cost-effective alternative, and the methodological contribution is better framed as a transparent mapping of the trade-off topology than as an algorithmic performance claim. Crucially, this reconciliation does not weaken the paper's central contribution, because that contribution is the modeling framework itself: the formalization of the informal-to-formal recycling transition as a three-objective problem with explicit policy levers, whose trade-off structure is then mapped and interrogated. The algorithm comparison in Section 4.2 is one component of the framework rather than its raison d'être, and the finding that a uniform sampler is competitive on a smooth, low-dimensional frontier is itself an informative policy-relevant result: it identifies when simple tools suffice and when evolutionary algorithms become necessary as the decision space grows (Section 5.4). The contribution, therefore, stands regardless of whether an evolutionary algorithm outperforms random search on this particular benchmark.

The hypervolume is reported on min–max normalized coordinates so that the three objectives, which differ in scale by several orders of magnitude ($f_1 \sim 10^3$, $f_2 \sim 10^{-1}$, $f_3 \sim 10^7$), are placed on a common dimensionless scale and a bounded reference region for reporting. Such normalization does not, by itself, alter the relative algorithm ordering, since a common per-axis affine rescaling multiplies every solution set's hypervolume by the same constant. Independently of this reporting choice, random search remains competitive on this problem (Section 4.2): it reaches a hypervolume comparable to or above the evolutionary algorithms despite consuming no algorithmic structure. This is a property of the problem rather than an artifact of metric construction, because the two-dimensional, smooth decision space imposes only weak modality and the benchmark uses equal evaluation budgets. Small differences in the Random-to-NSGA-II HV ratio between the original and rechecked comparisons (on the order of a few percentage points) arise from changes in the data pool (the random archive was truncated to 120 points in the original runs versus the full ~7000-point archive in the recheck) and from the reference point (a provisional estimate versus the shared non-dominated-front anti-ideal), not from the normalization step.

A methodological contribution worth highlighting is the deliberate simplicity of the model. The two-variable decision space converges within 50 generations for a population of 100, a finding that demonstrates the framework's accessibility to policy analysts without specialized optimization infrastructure rather than diminishing the value of MOEAs. As Papalexopoulos [31] argued, interpretable decision-support tools that make trade-off spaces transparent to non-technical stakeholders are at least as valuable as algorithmically sophisticated black-box optimizers in public policy contexts. The rapid convergence keeps the computational cost modest: the six experiments together comprise 503 optimization runs, with 30 independent runs per condition in the baseline, algorithm-comparison, and scenario experiments (Section 4.2) and fewer replicates per condition in the sensitivity analysis (Experimental Design section). This positions the framework as a policy modeling methodology in which MOEAs serve as an analytical tool for mapping trade-off topologies rather than merely to optimize.

The directional order-of-magnitude check (Section 3.7) illustrates that even a stylized model, with parameters set to order-of-magnitude consistency with publicly documented benchmarks, can produce policy-relevant insights. The representative compromise point's recycling rate of 44.5% is directionally consistent with classification-outcome improvements observed in Chinese megacities. This provides a form of face validity for the model as a deliberative tool, but it is a consistency check rather than a claim of quantitative predictive accuracy for any specific city; the model's parameters are stylized priors, not fitted estimates. A question that naturally arises is why the framework is not directly fitted to a particular city. Our answer is deliberate and twofold. First, the primary contribution is a *reproducible methodological template*, not a city-specific forecast: the model is designed so that its structure, objectives, and levers are transferable, and its parameters can be recalibrated against city-level panel data as those become available, allowing the stylized baseline to be refined into municipality-specific estimates without altering the model structure itself. Prematurely fitting to a single city would trade this generality for a localized accuracy that the available data (which are themselves partial, as the Beijing figures in Section 3.7 illustrate) could not reliably deliver. Second, by keeping parameters stylized and explicit, the model exposes rather than hides its assumptions, making the sensitivity of the policy frontier to each parameter transparent and actionable. The framework is, therefore, positioned as an extensible decision-support tool whose value lies precisely in being cheap to instantiate, easy to interrogate, and straightforward to re-fit as empirical estimates improve.

5.2. Policy Implications

The parameter sensitivity results (Section 4.3) identify γ_1, the formalization gain coefficient, as the parameter with the largest influence on HV within the examined ranges, which points to it as a priority empirical unknown. In practice, estimating γ_1 requires city-specific data on the incremental recycling volume achieved per unit increase in formalization. This calls for granular, longitudinal studies that track recycling rates before and after formalization interventions (e.g., the introduction of licensed recycling enterprises, the closure of informal dumpsites). The China case, with its rapid serial policy changes (2017 import ban, 2019–2020 classification mandates, 2024 vehicle licensing), offers a uniquely information-rich empirical setting for such estimation [5].

The compromise strategy (D) locates near-complete formalization ($\alpha \approx 0.97$) on the frontier at moderate enforcement intensity ($E \approx 0.33$). Because the model assigns no direct fiscal cost to formalization, near-complete formalization is attainable at low expenditure; this reflects a model assumption rather than an empirical claim. A subsidy dimension is excluded (Section 3.2.3), so the choice between subsidy and enforcement as policy instruments lies outside what this framework can arbitrate. What the model does speak to is the sensitivity of the frontier to the formalization gain coefficient: a lower γ_1 shifts the frontier toward lower formalization, since the marginal recycling return of formalization shrinks, while enforcement retains its role. Quantifying γ_1 empirically is the binding step for any policy application, particularly where informal networks are exceptionally efficient, as documented for Indian waste-picker cooperatives [17] and Brazilian *catador* organizations [46].

5.3. Addressing the Livelihood Framing

An important normative caveat applies to Objective 1, which is formulated as minimizing the waste-picker headcount. This framing could be interpreted as advocating for the elimination of informal livelihoods, a position at odds with the substantial literature documenting waste pickers as essential environmental service providers [17,18]. We, therefore, emphasize two limits of f_1. First, it is an *exit or displacement proxy*, not a measure of successful economic integration: the model assumes displaced workers are absorbed out of informal recycling via the exponential income term, but it tracks neither income nor occupational safety nor social protection, so a falling headcount cannot be equated with improved livelihoods. The empirical literature underscores this gap: in a global review of 45 waste-picker studies across 27 countries, formalization often failed to deliver the promised legal recognition, safe working conditions, and fair bargaining [47]; in Blantyre, Malawi, waste pickers were unlikely to self-organize into cooperatives given fears of income decline, free-riding, and loss of independence [48] and in two Colombian cities, formalization policies became mechanisms of material, spatial, and political dispossession rather than of integration [49]. Second, the headcount itself is dominated by the fixed income term: at reference GDP the absorption factor is $e^{-4} \approx 0.018$, so even at $\alpha = 0$ only about 366 of the 20,000 pre-absorption stock remain, and the formalization lever contributes only the further reduction from that baseline. Minimizing f_1 is thus best read as reducing residual informal employment, not as delivering integration success. Future extensions should incorporate a multidimensional livelihood metric that captures income, occupational safety, and social protection, rather than headcount alone [50]. We reiterate this distinction explicitly in relation to the model's objective structure: because the framework minimizes headcount without a benefit channel that rewards the income, safety, or social protection of displaced workers, a reduction in f_1 may merely reflect displacement of workers out of the informal sector rather than successful economic integration. The social objective should, therefore, be interpreted as an exit proxy, and any policy reading of the frontier that equates a falling headcount with improved welfare is out of scope for the present model. A multidimensional livelihood objective, combining income adequacy, occupational safety, and social-protection coverage of formalized workers, is a priority extension that requires data the stylized setting does not provide.

5.4. Limitations

Several limitations should be acknowledged. First, the present sensitivity analysis is a one-at-a-time (OAT) design over the examined ranges; a full global sensitivity analysis using Latin hypercube sampling with Sobol' variance decomposition would provide a more complete picture of higher-order parameter interactions and nonlinear effects. This extension is computationally modest given the problem's tractability and is planned for future work. Second, the stylized nature of the objective functions, while enabling transparency and interpretability, means that formal empirical calibration against city-level panel data is needed before the model can inform specific policy decisions for a particular municipality.

The directional order-of-magnitude check in Section 3.7 provides a consistency reference only and does not substitute for systematic calibration or confer city-level predictive validity. The rapid convergence of NSGA-II (within ∼50 generations) further suggests that the two-variable problem may be insufficiently challenging to stress-test algorithmic differences. This follows from the structural simplicity of the decision space rather than from the algorithms' capabilities: with only two effective policy levers and a smooth, convex frontier, the problem is tractable enough for a uniform sampler to compete with the evolutionary algorithms (Section 4.2). Consequently, the present model is insufficient as a benchmark for MOEA performance, and the near-parity of random search here should not be read as evidence against evolutionary search in general. Extending the model to 6–10 dimensions (e.g., spatial zoning, temporal phasing, differentiated waste streams) would provide a more rigorous testbed for algorithmic comparison. Third, the model treats all recycled materials homogeneously and does not differentiate waste streams (plastics, paper, metals, e-waste), each of which may exhibit distinct formalization dynamics [51]. This homogenization matters for both realism and policy relevance: distinct streams differ not only in their formalization dynamics but also in their recycling value, collection cost, and the ease with which they can be diverted into formal channels, so a stream-resolved model could reveal that some streams are worth formalizing early (high value, low displacement friction) while others are best left to the informal sector, and it could support stream-specific policy instruments (e.g., differentiated licensing or deposit schemes) rather than a single uniform formalization target. Incorporating differentiated waste streams is, therefore, a priority extension that would materially enhance the model's relevance to urban waste governance. Fourth, the subsidy dimension is excluded from the model, so it provides no evidence about whether subsidies outperform enforcement. Fifth, all fiscal quantities are reported in abstract model currency units rather than a specific currency or price year; they are comparable only within the model and should not be read as actual fiscal cost, budget ceilings, or shares of real GDP. The model also assigns no direct fiscal cost to formalization and tracks no social-protection or formal-employment outcomes, so it does not implement a full livelihood–fiscal–environmental trilemma. These are deliberate scoping choices that bound the framework's claims; testing the subsidy-versus-enforcement question would require positing and calibrating benefit channels for fiscal transfers.

5.5. Future Research Directions

Three extensions appear particularly promising. The first is **empirical calibration** using city-level panel data that links formalization policy changes to observed recycling rates and informal-sector employment. China's municipal-level waste statistics, combined with the WIEGO informal economy database [52] and remote sensing of informal settlements, could support a multi-city calibration exercise.

The second is **dynamic multi-objective optimization**, where the Pareto frontier evolves over time as GDP per capita, waste generation, and policy regimes change. A dynamic MOEA framework [21] could identify robust strategies that remain near-Pareto-optimal across multiple time periods, rather than optimizing for a single static snapshot.

The third is **spatial extension**: incorporating GIS data on waste generation hotspots, informal settlement locations, and recycling facility placement would transform the model from an aspatial policy simulation into a spatially explicit urban planning tool, along the lines of land-use MOEA frameworks [20].

The fourth extension addresses the subsidy dimension excluded from the present framework (Section 3.2.3). If subsidies were given a direct benefit channel, they would alter the Pareto frontier in a structurally different way from enforcement. In the current model, enforcement raises the recycling rate at a convex fiscal cost while leaving formalization to the planner, so the frontier is traced by the two levers α and E in a fixed (low-dimensional) lever space. A subsidy with an integration benefit channel, for example, transfers conditional on a picker joining a formal cooperative that also raises the recycling rate, would introduce a second cost-bearing instrument that trades fiscal expenditure against both f_1 and f_2. Because subsidy and enforcement would then compete for the same fiscal budget under the ceiling constraint, the feasible region would expand in the number of levers, and the frontier would in general shift outward (higher recycling and lower residual headcount for a given budget) whenever the subsidy's benefit per unit cost exceeds that of enforcement at the margin. The key qualitative change is that the frontier would cease to be convex in the single fiscal instrument: the crowding-out pattern currently attributed to enforcement alone would be reshaped by the relative cost-effectiveness of the two instruments, potentially flattening the frontier at low fiscal cost and changing the location of the compromise region where recycling gains saturate. Calibrating such a benefit channel requires cooperative-level data on formalization outcomes, which is not available for the stylized setting here; we, therefore, treat the subsidy-versus-enforcement comparison as a targeted extension rather than a claim of the present model.

6. Conclusions

This study proposed and demonstrated a multi-objective evolutionary optimization framework for the informal-to-formal recycling transition, formulated as a three-objective problem balancing residual informal waste-picker headcount (an exit/displacement proxy), recycling rates, and government expenditure. The four research questions posed in the Introduction are answered as follows.

RQ1 (Modeling). The informal-to-formal recycling transition can be formulated as a three-objective optimization problem driven by two effective policy levers, the formalization target α and the enforcement intensity E. Under the model, the social objective (residual informal waste-picker headcount f_1), the environmental objective (recycling rate f_2), and the fiscal objective (government expenditure f_3) form a genuine trade-off surface: formalization reduces residual informal employment and raises the recycling rate up to a crowding-out threshold, while enforcement raises the recycling rate at a convex fiscal cost, and the fiscal ceiling bounds the feasible region.

RQ2 (Algorithm). On this low-dimensional problem, no algorithm enjoys a decisive advantage: an unconstrained random search reaches a hypervolume comparable to or above both evolutionary algorithms, and the value of the evolutionary algorithms lies in their scalability as the decision space grows rather than in dominance at this dimensionality. Under the current configuration, SPEA2 attains a higher hypervolume and a more evenly spread frontier than NSGA-II, but these are per-metric, configuration-specific results that, as emphasized in the Methodological Contributions section, should not be generalized into a default-algorithm recommendation.

RQ3 (Sensitivity and scenarios). Within the examined one-at-a-time ranges, the formalization gain coefficient γ_1 exhibits the largest hypervolume coefficient of variation (CV = 13.2%), identifying it as the priority empirical unknown; the enforcement cost coefficient C_{enf} and the absorption elasticity λ are comparatively insensitive. Economic scenarios shift the Pareto frontier in distinct ways, with the boom scenario attaining the largest objective-space coverage under a shared hypervolume definition (HV $= 0.764$), consistent with the model's analytic dominance structure, and the recession scenario shifting the frontier toward larger waste-picker populations and lower recycling rates.

RQ4 (Ablation and policy). Bi-objective ablations confirm that only a small share of bi-objective solutions is strictly dominated in the full three-objective space (0.00–0.56%), indicating that the three objectives are largely independent; the hidden-cost implications of omitting an objective depend on the pairing and aggregation rule and are not established here. A representative compromise strategy chosen by the authors, with $\alpha \approx 0.97$ and $E \approx 0.33$, achieves a recycling rate of 44.5% with near-complete formalization at modest fiscal cost (3.2×10^7 model units), driven by the two effective levers; the subsidy dimension is excluded from the model.

The framework is intended as a stylized decision-support tool. Its primary value lies in making explicit the trade-offs among the objectives that the model implements and in generating a transparent, reproducible frontier of non-dominated alternatives for deliberation by policymakers, researchers, and civil-society stakeholders. The modeled levers are formalization and enforcement; the framework does not compare subsidies against enforcement, and its social objective is an exit/displacement headcount proxy without a social-protection or formal-employment channel. Because most of the headcount decline from the 20,000 pre-absorption stock to the low hundreds is attributable to the fixed income term rather than to the policy levers, reductions in f_1 should be read as reduced residual informal employment rather than as demonstrated livelihood improvement. All fiscal values are reported in abstract model currency units, so expenditure and budget figures are comparable only within the model.

Supplementary Materials: The following supporting information can be downloaded at https://www.mdpi.com/article/10.3390/su18179106/s1, Python source code for all experiments (`problem.py`, `experiment1_baseline.py` through `experiment5_2d_vs_3d.py`, `experiment6_policy.py`, `config.py`, `visualize.py`, and `utils.py`); raw Pareto-front CSV files and per-run numeric outputs for Experiments 1–5; the min–max normalized hypervolume comparisons for NSGA-II, SPEA2, and random search and all figures in PDF vector format. Complete per-experiment replication structures are detailed in the Experimental Design section; the numerical outputs underlying each optimization run, rather than full console transcripts, are archived for all 503 runs.

Author Contributions: Conceptualization, X.Z.; methodology, X.Z.; software, X.Z.; formal analysis, X.Z.; investigation, X.Z.; data curation, X.Z.; writing—original draft preparation, X.Z.; writing—review and editing, T.W. and J.H.; visualization, X.Z.; supervision, T.W. and J.H.; funding acquisition, T.W. All authors have read and agreed to the published version of the manuscript.

Funding: This work was funded by the Natural Science Foundation of Hubei Province, grant number 2026AFC0066 (T.W.).

Institutional Review Board Statement: Not applicable.

Informed Consent Statement: Not applicable.

Data Availability Statement: The data and code supporting the reported results are permanently archived at https://doi.org/10.5281/zenodo.21860082 (accessed on 30 August 2026) (GitHub: https://github.com/tinyboy1993/Informal_waste_economy (accessed on 30 August 2026)), which includes the Pareto-front CSV files, performance metrics, per-run numeric outputs, and figures. No proprietary or human-subject data were used in this study.

Acknowledgments: The author is grateful to a colleague who provided constructive feedback on an earlier draft of this manuscript. The author also acknowledges the open-source `pymoo` framework [43] that facilitated the computational experiments, and the WIEGO network for maintaining the informal economy statistical database.

Conflicts of Interest: The author declares no conflicts of interest.

Abbreviations

The following abbreviations are used in this manuscript:

MOEA	Multi-Objective Evolutionary Algorithm
NSGA-II	Non-dominated Sorting Genetic Algorithm II
SPEA2	Strength Pareto Evolutionary Algorithm 2
HV	Hypervolume
IGD	Inverted Generational Distance
MSW	Municipal Solid Waste
CV	Coefficient of Variation
OAT	One-at-a-Time (sensitivity analysis)

References

1. Cook, E.; Cano, N.S.S.L.; Velis, C.A. Informal recycling sector contribution to plastic pollution mitigation: A systematic scoping review and quantitative analysis of prevalence and productivity. *Resour. Conserv. Recycl.* **2024**, *207*, 107588. [CrossRef]
2. Linzner, R.; Lange, U. Role and size of informal sector in waste management: A review. *Proc. Inst. Civ. Eng.-Waste Resour. Manag.* **2013**, *166* , 69–83. [CrossRef]
3. Velis, C.A.; Hardesty, B.D.; Cottom, J.W.; Wilcox, C. Enabling the informal recycling sector to prevent plastic pollution and deliver an inclusive circular economy. *Environ. Sci. Policy* **2022**, *138*, 20–25. [CrossRef]
4. Buch, R.; Marseille, A.; Williams, M.; Aggarwal, R.; Sharma, A. From waste pickers to producers: An inclusive circular economy solution through development of cooperatives in waste management. *Sustainability* **2021**, *13*, 8925. [CrossRef]
5. Chen, G.; Feng, J.; Chen, L. Dharavi in Beijing? A hidden geography of waste and migrant exclusion. *Prof. Geogr.* **2023**, *75*, 102–115. [CrossRef]
6. Liu, T.; Wu, Y.; Tian, X.; Gong, Y. Urban household solid waste generation and collection in Beijing, China. *Resour. Conserv. Recycl.* **2015**, *104*, 31–37. [CrossRef]
7. Tong, Y.D.; Huynh, T.D.X.; Khong, T.D. Understanding the role of informal sector for sustainable development of municipal solid waste management system: A case study in Vietnam. *Waste Manag.* **2021**, *124*, 118–127. [CrossRef]
8. Aleluia, J.; Ferrão, P. Characterization of urban waste management practices in developing Asian countries: A new analytical framework based on waste characteristics and urban dimension. *Waste Manag.* **2016**, *58*, 415–429. [CrossRef]
9. Matter, A.; Dietschi, M.; Zurbrügg, C. Improving the informal recycling sector through segregation of waste in the household: The case of Dhaka Bangladesh. *Habitat Int.* **2013**, *38*, 150–156. [CrossRef]
10. Steuer, B. Is China's regulatory system on urban household waste collection effective? An evidence-based analysis on the evolution of formal rules and contravening informal practices. *J. Chin. Gov.* **2017**, *2*, 411–436. [CrossRef]
11. Guabiroba, R.C.S.; Jacobi, P.R.; Besen, G.R.; da Silva, M.A.V. Sustainability performance indicators: Improving waste picker organizations in a Brazilian region. *J. Mater. Cycles Waste Manag.* **2024**, *26*, 3492–3507. [CrossRef]
12. Moreno-Sanchez, R.; Maldonado, J.H.; Sheldon, I. The Role of Informal Waste-Pickers in a Dynamic Model of Solid-Waste Disposal and Recycling in Developing Countries. 2004. Available online: https://www.researchgate.net/publication/228780527_The_role_of_informal_waste-pickers_in_a_dynamic_model_of_solid-waste_disposal_and_recycling_in_developing_countries (accessed on 30 August 2026).
13. Gutberlet, J. Grassroots waste picker organizations addressing the UN sustainable development goals. *World Dev.* **2021**, *138*, 105195. [CrossRef]
14. Gómez-Maldonado, A.; Ospina-Espita, L.C.; Rodríguez-Lesmes, P.; Rodríguez-Rodriguez, M.A. Barriers and opportunities for waste pickers within solid waste management policy in Colombia. *Waste Manag.* **2023**, *163*, 1–11. [CrossRef]
15. Rateau, M.; Tovar, L. Formalization of wastepickers in Bogota and Lima: Recognize, regulate, and then integrate? *EchoGéo* **2019**, 47. [CrossRef]
16. Zisopoulos, F.K.; Steuer, B.; Abussafy, R.; Toboso-Chavero, S.; Liu, Z.; Tong, X.; Schraven, D. Informal recyclers as stakeholders in a circular economy. *J. Clean. Prod.* **2023**, *415*, 137894. [CrossRef]
17. Gidwani, V. The work of waste: Inside India's infra-economy. *Trans. Inst. Br. Geogr.* **2015**, *40*, 575–595. [CrossRef]
18. Nzeadibe, T.C.; Anyadike, R.N.C.; Njoku-Tony, R.F. A mixed methods approach to vulnerability and quality of life assessment of waste picking in urban Nigeria. *Appl. Res. Qual. Life* **2012**, *7*, 351–370. [CrossRef]
19. Mbah, P.O.; Nzeadibe, T.C. Inclusive municipal solid waste management policy in Nigeria: Engaging the informal economy in post-2015 development agenda. *Local Environ.* **2017**, *22*, 203–218. [CrossRef]
20. Sicuaio, T.; Zhao, P.; Pilesjö, P.; Shindyapin, A.; Mansourian, A. Sustainable and resilient land use planning: A multi-objective optimization approach. *ISPRS Int. J. Geo-Inf.* **2024**, *13*, 99. [CrossRef]

21. Chen, Y.F.; Chan, W.H.; Su, E.L.M.; Diao, Q. Multi-objective optimization for smart cities: A systematic review of algorithms, challenges, and future directions. *PeerJ Comput. Sci.* **2025**, *11*, e3042. [CrossRef]
22. Raimbault, J.; Pumain, D. Trade-offs between sustainable development goals in systems of cities. *J. Urban Manag.* **2022**, *11*, 237–251. [CrossRef]
23. Yu, H.; Solvang, W.D. A multi-objective location-allocation optimization for sustainable management of municipal solid waste. *Environ. Syst. Decis.* **2017**, *37*, 289–308. [CrossRef]
24. Hernández-Romero, I.M.; Niño-Caballero, J.C.; González, L.T.; Pérez-Rodríguez, M.; Flores-Tlacuahuac, A.; Montesinos-Castellanos, A. Waste management optimization with NLP modeling and waste-to-energy in a circular economy. *Sci. Rep.* **2024**, *14*, 19922. [CrossRef]
25. Habibi, F.; Asadi, E.; Sadjadi, S.J.; Barzinpour, F. A multi-objective robust optimization model for site-selection and capacity allocation of municipal solid waste facilities: A case study in Tehran. *J. Clean. Prod.* **2017**, *166*, 816–834. [CrossRef]
26. Ahani, M.; Arjmandi, R.; Hoveidi, H.; Ghodousi, J.; Miri Lavasani, M.R. A multi-objective optimization model for municipal waste management system in Tehran city, Iran. *Int. J. Environ. Sci. Technol.* **2019**, *16*, 5447–5462. [CrossRef]
27. Farrokhi-Asl, H.; Tavakkoli-Moghaddam, R.; Asgarian, B.; Sangari, E. Metaheuristics for a bi-objective location-routing-problem in waste collection management. *J. Ind. Prod. Eng.* **2017**, *34*, 239–252. [CrossRef]
28. Zhou, J.; Zhang, M.; Wu, S. Multi-objective vehicle routing problem for waste classification and collection with sustainable concerns: The case of Shanghai City. *Sustainability* **2022**, *14*, 11498. [CrossRef]
29. Ibanez, E.; McCalley, J.D. Multiobjective evolutionary algorithm for long-term planning of the national energy and transportation systems. *Energy Syst.* **2011**, *2*, 151–169. [CrossRef]
30. He, Z.; Wang, J.; Huang, J.; Du, M. Spatiotemporal evolution and nonlinear explanatory factors of landscape ecological risk and ecosystem service value in the Ordos Plateau. *Land* **2026**, *15*, 1224. [CrossRef]
31. Papalexopoulos, T.P. Multi-objective optimization for public policy. Master's Thesis, Massachusetts Institute of Technology, Cambridge, MA, USA, 2022.
32. Liu, D.X.; Gu, Y.R.; Qian, C.; Mu, X.; Tang, K. Migrant resettlement by evolutionary multi-objective optimization. *IEEE Trans. Artif. Intell.* **2025**, *6*, 51–65. [CrossRef]
33. Guo, Y.; Wei, R.; Zhang, X.; Chai, F.; Zhao, Y.; Zhou, T. Positive impacts of the overall-process management measures on promoting municipal solid waste classification: A case study of Chongqing, China. *Sustainability* **2022**, *14*, 14250. [CrossRef]
34. Alharbi, S.T. Multi-objective evolutionary algorithms in waste disposal systems: A comprehensive review of applications, case studies, and future directions. *Computers* **2025**, *14*, 316. [CrossRef]
35. Shi, J.; Wang, R.; Chen, W.; Xing, L.; Jin, M. Bi-objective design of household E-waste collection with public advertising and competition from informal sectors. *Waste Manag.* **2020**, *102*, 65–75. [CrossRef]
36. Peña, D.A.; Montoya-Torres, J.R.; Amodeo, L. A sustainable two-echelon waste collection routing: Understanding waste picker behavior. *Socio-Econ. Plan. Sci.* **2025**, *102*, 102288. [CrossRef]
37. Kusi-Appiah, M.; Liu, L.; Murphy, R.J.; Zarei, A. Optimising integrated solid waste management (ISWM) system under seasonal variations. *Environ. Syst. Res.* **2026**, *15*, 9. [CrossRef]
38. Wang, Y.; Shi, Y.; Zhou, J.; Zhao, J.; Maraseni, T.; Qian, G. Implementation effect of municipal solid waste mandatory sorting policy in Shanghai. *J. Environ. Manag.* **2021**, *298*, 113512. [CrossRef]
39. Zhang, H.; Wen, Z.G. The consumption and recycling collection system of PET bottles: A case study of Beijing, China. *Waste Manag.* **2014**, *34*, 987–998. [CrossRef]
40. Orlins, S.; Guan, D. China's toxic informal e-waste recycling: Local approaches to a global environmental problem. *J. Clean. Prod.* **2016**, *114*, 71–80. [CrossRef]
41. Deb, K.; Pratap, A.; Agarwal, S.; Meyarivan, T. A fast and elitist multiobjective genetic algorithm: NSGA-II. *IEEE Trans. Evol. Comput.* **2002**, *6*, 182–197. [CrossRef]
42. Zitzler, E.; Laumanns, M.; Thiele, L. SPEA2: Improving the strength Pareto evolutionary algorithm. *Tik-Rep. Eth Zur.* **2001**, *103*, 1–21.
43. Blank, J.; Deb, K. Pymoo: Multi-objective optimization in Python. *IEEE Access* **2020**, *8*, 89497–89509. [CrossRef]
44. Liu, X.; Fu, H.; Jiang, H.; Shao, Y.; Wu, X.; Li, Z. A survey of municipal solid waste landfills in Beijing during 2009–2011. *Environ. Sci. Pollut. Res.* **2019**, *26*, 20286–20296. [CrossRef]
45. Linzner, R.; Salhofer, S. Municipal solid waste recycling and the significance of informal sector in urban China. *Waste Manag. Res.* **2014**, *32*, 896–907. [CrossRef]
46. Maiello, A. In, out or beyond? Waste pickers and policy networks: A story from Jardim Gramacho (Rio de Janeiro). *Sustainability* **2022**, *14*, 16977. [CrossRef]
47. Morais, J.; Corder, G.; Golev, A.; Lawson, L.; Ali, S. Global review of human waste-picking and its contribution to poverty alleviation and a circular economy. *Environ. Res. Lett.* **2022**, *17*, 6. [CrossRef]

48. Kasinja, C.; Tilley, E. Formalization of Informal Waste Pickers' Cooperatives in Blantyre, Malawi: A Feasibility Assessment. *Sustainability* **2018**, *10*, 1149. [CrossRef]
49. Neville, L.; Tovar Cortés, L.F. Waste Pickers' Formalisation from Bogotá to Cartagena de Indias: Dispossession and Socio-Economic Enclosures in Two Colombian Cities. *Sustainability* **2023**, *15*, 9047. [CrossRef]
50. Blaauw, P.; Pretorius, A.; Viljoen, K.; Schenck, R. Adaptive expectations and subjective well-being of landfill waste pickers in South Africa's Free State Province. *Urban Forum* **2020**, *31*, 135–155. [CrossRef]
51. Valente, D.B.; Guabiroba, R.C.S.; Conejero, M.A.; da Silva, M.A.V.; César, A.S. Economic analysis of waste electrical and electronic equipment management: A study involving recycling cooperatives in Brazil. *Environ. Dev. Sustain.* **2021**, *23*, 17628–17649. [CrossRef]
52. Chikarmane, P.; Narayanan, L. Statistics on Waste Pickers: A Case Studies Guide. WIEGO Statistical Brief No. 39. 2024. Available online: https://www.wiego.org/research-library-publications/statistics-waste-pickers-case-studies-guide/ (accessed on 26 July 2026).